10ème Congrès Français d'Acoustique

Lyon, 12-16 Avril 2010

Numerical Experiments with Coupled Membranes and the Snare Mechanism

Stefan Bilbao[1]

[1] Acoustics and Fluid Dynamics Group/Music, University of Edinburgh, sbilbao@staffmail.ed.ac.uk

The snare drum is one of the more complex musical instruments from a modeling and synthesis perspective—it includes elements modeled as 0D (the drum stick), 1D (the snares), 2D (a pair of membranes) and 3D (the cavity and perhaps the surrounding space), as well as connection conditions, including the distributed collision between the set of snares and the snare head.

In this article, some preliminary modeling results will be presented, employing time-domain finite difference schemes for the membranes and snare set, and various different levels of modeling for the adjacent acoustic space, including a full 3D model involving absorbing boundary conditions.

Simulation results and sound examples will be presented, and computational complexity wil be discussed.

1 Introduction

Simulation based on physical models of musical instruments, both for investigation in musical acoustics, and in sound synthesis applications, has developed enormously in recent years; some of the more interesting new directions have involved the simulation of complex structures, with multiple interacting components, normally distributed. Among the structures examined, from the point of view of musical acoustics, have been the kettledrum [9], and, in synthesis, the piano, including models of the interaction between the strings and the soundboard and sympathetic vibration [14], and, the subject under study here, drums which employ two membranes as well as a snare mechanism [8]. Great recent increases in computational power have made it possible to generate synthetic sound in real time, or something approaching real time.

Modal approaches are often used when when the behaviour of the object under study is very nearly linear; when nonlinearities are present, such an approach quickly becomes unwieldy; time domain methods, while moderately more expensive computationally, become an attractive option. Such is the case for the snare drum, composed of a cavity, enclosed by two membranes, one of which is in distributed partial contact with a set of snares. Though the literature on the snare drum is sparse, a good experimental account may be found in [10], and synthesis techniques are discussed in [8]. On the other hand, time domain methods present their own special problems—and the numerical issues are many, especially with regard to adequate sound rendering for synthesis.

In this short paper, some preliminary simulation results based on a coupled membrane model of a snare drum are presented. In Section 2, a basic model is presented (with indications as to how it may be extended to include more realistic features), and in Section 3, a system of finite difference schemes for the various components is presented, accompanied by a brief discussion of computational complexity. Numerical results appear in Section 4.

2 Model Description

In this study, the snare drum is assumed to be a cylinder, of radius R metres, and of depth L metres. The entire problem is embedded within a 3D computational domain D of the form of a parallelipiped, with $D = \{(x, y, z) \in \mathbb{R}^3 | -L_{xy}/2 \leq x, y \leq L_{xy}/2, -L_z/2 \leq z \leq L_z/2\}$. The six outer faces of the region will be denoted, collectively, as ∂D_{outer}.

The shell of the drum, defined over the region $\partial D_{shell} = \{(x, y, z) \in \mathbb{R}^3 | x^2 + y^2 = R^2, -L/2 \leq z \leq L/2\}$, is assumed to be perfectly rigid. Flexible membranes terminate the cylinder over regions $\partial D_v = \{(x, y, z) \in \mathbb{R}^3 | x^2 + y^2 \leq R^2, z = L/2\}$ (for the batter head) and $\partial D_w = \{(x, y, z) \in \mathbb{R}^3 | x^2 + y^2 \leq R^2, z = -L/2\}$ (for the snare head). See Figure 1.

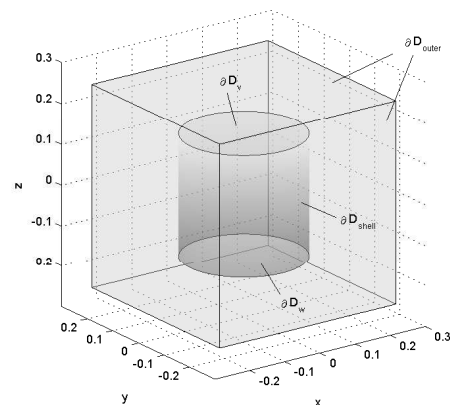Figure 1: Drum geometry and computational space.

2.1 Acoustic Space, and Boundary Conditions

The acoustic space, defined over the region D, including both the interior of the drum cavity and outside, is assumed described by the linear 3D wave equation,

$$\Psi_{tt} = c^2 \Delta^{(3)} \Psi \tag{1}$$

Here, c is the wave speed in air, $\Delta^{(3)}$ is the 3D Laplacian, defined, in Cartesian coordinates, by

$$\Delta^{(3)} = \frac{\partial^2}{\partial x^2} + \frac{\partial^2}{\partial y^2} + \frac{\partial^2}{\partial z^2} \tag{2}$$

and subscripts t indicate partial time differentiation. The quantity $\Psi(x, y, z, t)$ is a velocity potential, which may be related to pressure p and velocity u by

$$p = \rho \Psi_t \qquad u = -\nabla \Psi \tag{3}$$

where ρ is air density. Working with the velocity potential, instead of a similar equation in the pressure itself makes for a much simplified stability/boundary condition analysis in the numerical setting, much as in the 1D case—see [4] for details.

At the boundary with the rigid shell, at ∂D_{shell}, both inside the drum cavity and outside, a Neumann (rigid) condition is employed:

$$\Psi_n = 0$$

where the subscript n indicates a spatial derivative of Ψ normal to ∂D_{shell}.

Over the boundary region ∂D_{outer}, an absorbing boundary condition of the form of one given in the article by Engquist and Majda [6], extended to 3D, such as

$$\Psi_t - c\Psi_n = 0$$
$$\Psi_{tt} - c\Psi_{nt} - \frac{c^2}{2} \left(\Psi_{s_1 s_1} + \Psi_{s_2 s_2} \right) = 0$$

where n indicates a derivative in a direction normal to the boundary, and where s_1 and s_2 are orthogonal coordinates tangential to the boundary.

Such conditions offer a simple alternative to more involved PML type conditions [2, 1], which require a 3D boundary region to be appended to the computational domain; to what order one must take such conditions to attenuate numerical reflections to perceptually minimal levels in audio applications remains an open question.

2.2 Membranes

The two membranes are assumed defined, by some extension of the 2D wave equation of the form

$$\rho_{M,v} H v_{tt} = T_v \Delta^{(2)} v + \ldots + f_v^{(+)} + f_v^{(-)} + f_e \tag{4a}$$
$$\rho_{M,w} H w_{tt} = T_w \Delta^{(2)} w + \ldots + f_w^{(+)} + f_w^{(-)} + f_s \tag{4b}$$

corresponding to the upper and lower membranes, respectively, over the regions ∂D_u and ∂D_w, respectively. Here $v = v(x, y, t)$ and $w = w(x, y, t)$ are the transverse displacements of the membranes, $\Delta^{(2)}$ is the 2D Laplacian, defined, in Cartesian coordinates, by

$$\Delta^{(2)} = \frac{\partial^2}{\partial x^2} + \frac{\partial^2}{\partial y^2} \tag{5}$$

$\rho_{M,v}$ and $\rho_{M,w}$ are the mass densities of the upper and lower membranes, and H is the membrane thickness. The terms $f^{(+)}$ and $f^{(-)}$ represent pressures on the upper and lower faces of the membranes, due to interaction with the surrounding acoustic space, and will be related to Ψ shortly, in Section 2.5. The term f_e (on the batter head of the drum) is an excitation term, due to mallet interaction. The full form of this term will be given in Section 2.3. Similarly, f_s represents the forces exerted on the bottom membrane by the snares, to be described in Section 2.4.

The two instances of ... represent other terms which may be added to give a much more realistic membrane model. These include a stiffness term, loss terms, and, possibly, a term yielding nonlinear behaviour along the lines of the model developed initially by Berger [3]. Due to space considerations, these will not be presented explicitly here—see [8] for more details.

The membranes are assumed to be rigidly terminated, i.e., $v = w = 0$ over $x^2 + y^2 = R^2$.

2.3 Striking Model

The striking model employed here is a crude model of a drumstick in freefall, and is similar to other such models of hammer or mallet interaction which appear in the literature [5, 9]. The excitation term f_e may be modelled as $f_e = -\delta^{(2)}(x-x_i, y-y_i) f_{stick}$, where $\delta^{(2)}(x-x_i, y-y_i)$ is a 2D Dirac delta function centered at $x = x_i, y = y_i$ (which could be generalized to a region of non-zero area), and where the stick force f_{stick} will be given by

$$f_{stick} = K_h \left([v(x_i, y_i) - m(t)]^+ \right)^{\alpha_h} \qquad \frac{d^2 m}{dt^2} = f_{stick} - g \tag{6}$$

where here, $m = m(t)$ is the vertical position of the stick relative to the upper membrane at location (x_i, y_i), and where K_h is a stiffness constant, α_h is a nonlinearity exponent, and $g = 9.8$ m/s^2. The superscript $^+$ indicates "the positive part of." Such a model should, eventually, be extended to include an applied force from the player.

2.4 Snare Model

In a typical snare drum, there are approximately 12 to 15 individual snares, which are fairly loosely tensioned wires (helical) which are pressed agains the bottom face of the snare head (whose transverse displacement here is w). For simplicity, an individual snare (one among M) will be modelled here as an ideal string:

$$\rho_s A_s r_{tt}^{(i)} = T_s r_{\eta^{(i)} \eta^{(i)}}^{(i)} + f^{(i)} \tag{7}$$

where $r^{(i)}$ is the transeverse displacement of the ith snare, $i = 1, \ldots, M$ (assumed normal to the lower membrane region ∂D_w), and where ρ_s, A_s and T_s are the mass density, effective cross-sectional area, and applied tension in the snares (assumed uniform over all snares). The coordinate η is some affine combination $\eta^{(i)} = a^{(i)} x + b^{(i)} y + c^{(i)}$, defining a linear region over ∂D_w.

The force $f^{(i)}$ on the ith snare is modelled as a distributed collision with the lower membrane, in a manner

similar to the hammer:

$$f^{(i)} = -K_s \left([r^{(i)} - w(\eta^{(i)})]^+ \right)^{\alpha_s}$$

where again, K_s is a stiffness constant, α_s is a nonlinearity exponent. The total force f_s exerted on the lower membrane will be

$$f_s = \sum_{i=1}^{M} \delta(\eta^{(i)} - a^{(i)}x + b^{(i)}y + c^{(i)})f^{(i)}$$

2.5 Connection Conditions

More subtle conditions are required in order to relate the acoustic field to to the membrane displacements over the regions ∂D_v and ∂D_w. These may be given as:

$$f_{v,w}^{(+)} = -\rho\Psi_t^{(+)}\Big|_{\partial D_{v,w}} \quad f_{v,w}^{(-)} = \rho\Psi_t^{(-)}\Big|_{\partial D_{v,w}} \quad (8)$$

$$v_t, w_t = -\Psi_z^{(+)}\Big|_{\partial D_{v,w}} = -\Psi_z^{(-)}\Big|_{\partial D_{v,w}} \quad (9)$$

where $\Psi^{(+)}$ and $\Psi^{(-)}$ indicate the values taken by Ψ on the upper and lower sides of the membranes, respectively.

3 Finite Difference Schemes

There is not space available here for a full introduction to finite difference schemes—see [11, 4] for a complete presentation. A cursory description of some basic operations follows.

In an audio synthesis setting (as opposed, perhaps, to investigations in pure musical acoustics), it is useful to choose a sample rate f_0 a priori, implying a time step $k = 1/f_0$. This time step will be used uniformly over all components. The choice of a uniform time step is by no means a necessary one, but leads to great simplifications in terms of implementation. A grid function f^n represents an approximation to some function $f(\ldots, t)$ at times $t = nk$. The symbol $\cdot$ refers to other spatial grid indices. The simplest approximation to a second time derivative is:

$$\delta_{tt}f_{\cdot} = \frac{1}{k^2}\left(f_{\cdot}^{n+1} - 2f_{\cdot}^n + f_{\cdot}^{n-1}\right) \approx f_{tt}(\ldots, t) \quad (10)$$

This approximation is second order accurate, and will lead (in conjunction with spatial discretization) to a certain amount of numerical dispersion [4].

The systems (1), for 3D acoustics, (4) for the membranes, and (7) for the snares are all variants of the wave equation, and as such, are easily approached using very simple schemes of the FDTD variety [13, 12]. The key operator to be discretized is the d dimensional Laplacian $\Delta^{(d)}$. First assume that all spatial coordinates are discretized, according to a Cartesian grid, using a spacing

h. The simplest approximations to the Laplacian are

$$\delta_{\Delta^{(1)},h}f_l^n = \frac{1}{h^2}\left(f_{l+1}^n - 2f_l^n + f_{l-1}^n\right)$$

$$\delta_{\Delta^{(2)},h}f_{l,m}^n = \frac{1}{h^2}\big(f_{l+1,m}^n + f_{l-1,m}^n + f_{l,m+1}^n + f_{l,m-1}^n - 4f_{l,m}^n\big)$$

$$\delta_{\Delta^{(3)},h}f_{l,m,p}^n = \frac{1}{h^2}\big(f_{l+1,m,p}^n + f_{l-1,m,p}^n + f_{l,m+1,p}^n + f_{l,m-1,p}^n + f_{l,m,p+1}^n + f_{l,m,p-1}^n - 6f_{l,m,p}^n\big)$$

Here, the indeces l, m and p refer to grid locations with coordinates $x = lh$, $y = mh$, $z = ph$.

3.1 Explicit Schemes

Simple explicit schemes corresponding to the various systems are then:

$$\delta_{tt}\Psi = c^2\delta_{\Delta^{(3)},h}\Psi \quad (11)$$

$$\rho_{M,v}A\delta_{tt}v = T_v\delta_{\Delta^{(2)},h_v}v + f_v^{(+)} + f_v^{(-)} + f_e \quad (12a)$$

$$\rho_{M,w}A\delta_{tt}w = T_w\delta_{\Delta^{(2)},h_w}w + f_w^{(+)} + f_w^{(-)} + f_s \quad (12b)$$

$$\rho_s A_s\delta_{tt}r^{(i)} = T_s\delta_{\Delta^{(2)},h_s}r^{(i)} + f^{(i)} \quad (13)$$

The grid spacings, h for the 3D system, h_v and h_w for the upper and lower membranes, and h_s for the snares are distinct here; for these explicit schemes, necessary stability conditions may be derived either from frequency domain analysis [11], or energy methods [4]. These are:

$$h \geq \sqrt{3}ck \quad (14a)$$

$$h_v \geq \sqrt{\frac{2T_v}{\rho_{M,v}H}}k \quad h_w \geq \sqrt{\frac{2T_w}{\rho_{M,w}H}}k \quad (14b)$$

$$h_s \geq \sqrt{\frac{T_s}{\rho_s A_s}}k \quad (14c)$$

In fact, if the spacings are not chosen very close to these bounds, severe numerical dispersion (and bandlimiting) will result, so for synthesis purposes, it is useful to keep these quantities separate, even though such a choice will entail extra complications when the various components necessarily interact. When other terms intervene (typically involving stiffness, in the case of membranes or snares, or frequency dependent loss), such conditions must be altered slightly [4], but will always take the form of a lower bound on the grid spacing, at least when an explicit scheme is used.

3.2 Grid Boundaries and Interpolation

The difficulties in the above framework, employing regular Cartesian grids are two-fold. First, compared with methods using unstructured grids (such as, e.g., finite element or finite volume methods), special boundary difference schemes must be developed at curved boundaries

(such as at the edges of the membranes, or at the faces of the drum cylinder) [7]. More general difficulties, especially lie in the distributed connection conditions between the membranes and the acoustic space, and between the snares and the lower membrane. Though the treatment of an individual component becomes simpler when a uniform grid is used, the distinct grid spacings require some form of interpolation—see Figure 2. A simple choice is of some form of linear or bilinear interpolation, relating vaues on one grid to those of nearest neighbours on the other. For more on interpolation between grids, see [4].

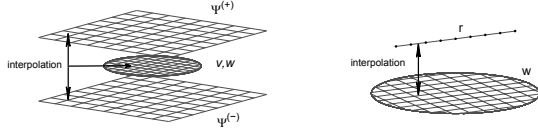
Figure 2: Grid interpolation: Left, between 3D acoustic spaces and membranes, and right, between snares and membrane.

3.3 Computational Complexity

Computational cost is dominated by the solution of the 3D wave equation over the domain D. If scheme (11) is used, with a time step k, and with grid spacing h chosen as close to the stability condition (14a) as possible (in order to minimize numerical dispersion and maximize output bandwidth, as discussed above), then the total memory requirement will be, for a two-step scheme,

$$\text{Memory Requirement}: \qquad 2\frac{L_{xy}^2 L_z}{3^{3/2}c^3 k^3}$$

and the total operation count (additions + multiplications/second) will be

$$\text{Operation Count}: \qquad \frac{10L_{xy}^2 L_z}{3^{3/2}c^3 k^4}$$

For a typical region including a snare drum, such as $L_{xy} = L_z = 0.5$, and operating at the sample rate $f_s = 44.1$ kHz, the total memory requirement will be approximately 8×10^6 floating point numbers, and the operation count will be approximately 10^{11} flops. This is large, but not enormous—one should expect to be able to perform such calculations in something approaching real time in the next few years, perhaps using general purpose graphics processing units (GPGPUs), or by exploiting parallelism and multi-core architectures. Computational cost can obviously be greatly reduced through operation at a lower sample rate, or by reducing the size of the computational region D—signifying perhaps the need for more accuracy in the reflectionless boundary layer.

4 Numerical Results

As a simple demonstration of the algorithm proposed here, snapshots of the time evolution of the two coupled membranes, where the upper membrane is subjected to a short impulsive excitation, is shown in Figure 3; a cross-section of the radiated pressure field is shown in Figure 4. In the last panel of this figure, the effect of the absorbing boundary conditions is clearly visible.
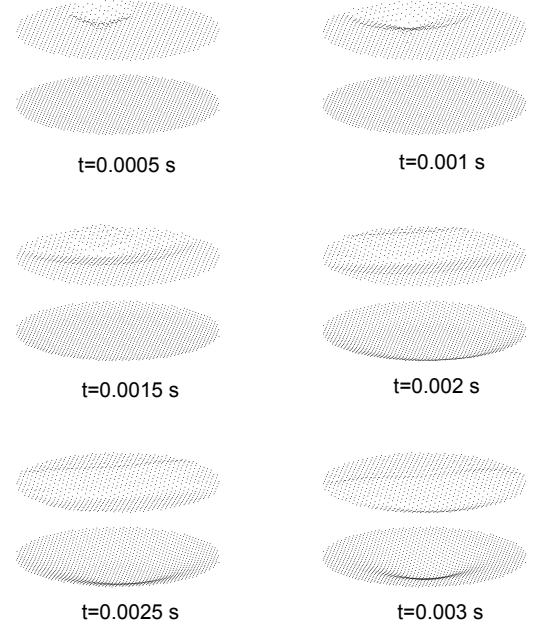

Figure 3: Snapshots of the time evolution of a coupled membrane system, at times as indicated. The upper and lower membranes have wave speeds of 95.2 m/s and 75.9 m/s, respectively, and are of radius 0.15 m. The cavity between them is of depth 0.3 m. The scheme described in Section 3 is used, at a sample rate of 16 kHz.

4.1 Membrane Mode Accuracy and Numerical Mode Splitting

At an audio sample rate, such as 44.1 kHz, mode accuracy using a regular FD scheme is very good; see Figure 5, illustrating the case of an isolated membrane, for which numerical mode frequencies differ from exact values by no more than 4 Hz over the band (0 3000)Hz.

One interesting defect of an FD approach, on a regular Cartesian grid applied to a circular problem is that of numerical mode splitting; because the grid does not possess rotational symmetry, degenerate modes may be split, as shown at right in Figure 5—the degree of splitting increases with frequency, and may be audible as a low frequency beating. One could remedy this with recourse to a polar grid, but at the cost of greatly increased numerical dispersion (and far inferior mode accuracy). On the other hand, given the high degree of inharmonicity of the spectrum of membrane, such effects are not nearly as important, perceptually, as they would be in the case of structures exhibiting a highly harmonic spectrum.
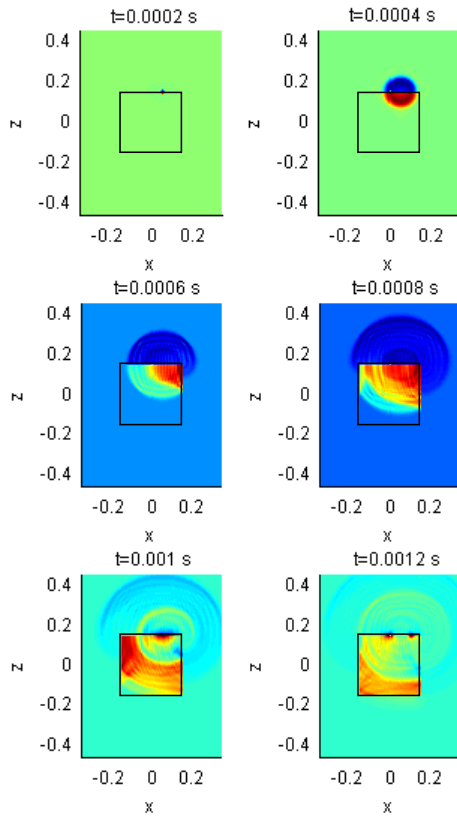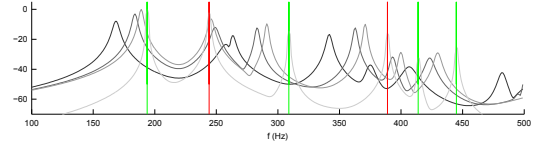
Figure 6: Output spectrum, read from a point on the lower membrane, to an impulsive excitation on the upper membrane, for different mass densities of the membranes (of wave speeds as indicated in the caption to Figure 3). Modal frequencies of the upper/lower membranes are indicated in red and green, respectively. Frequency response curves, drawn from displacement at the bottom membrane, are indicated with for relative mass densities of 1 (dark), 2, 3 and 1000 (light grey), with nominal densities of 0.33 kg/m² and 0.26 kg/m² for the upper and lower membranes respectively.

followed, eventually, by a nearly randomized motion of the snares. As expected, this leads to a noise-like quality in sound output, as illustrated in Figure 8.

Figure 4: Snapshots of a vertical cross-section of the pressure distribution surrounding a coupled membrane/cavity system, at times as indicated. A high sample rate of 80 kHz is used, for increased spatial resolution.
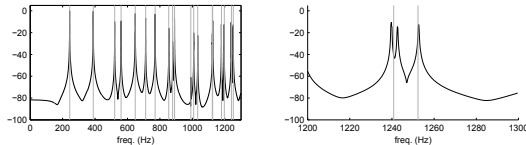
Figure 5: Frequency response for a finite difference membrane with wave speed 95.65 m/s, and radius 0.15 m, at 44.1 kHz. Left: Response for a single membrane, in black, and exact modal frequencies, in grey. Right: a numerically split mode near 1240 Hz.

4.2 Coupled Membranes, and Modal Frequencies

The subject of modal frequency shifts due to air coupling between membranes has been touched upon in [10], specifically with reference to a two-mass piston model of the air within the cavity. Here, however, the cavity is modelled in its entirety, and one may observe modal frequency shifts in all modal frequencies, and not merely those which possess axisymmetry. See Figure 6.

4.3 Snare Interaction

The interaction of the snares with the lower membrane is enormously complex—see Figure 7, illustrating the initial deformation of the membrane due to the snares,
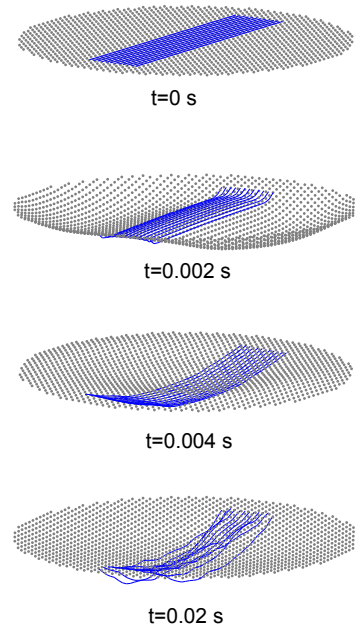

Figure 7: Snapshots of interaction of twelve snares with lower membrane, for a strike applied to the upper membrane, at times as indicated. The sample rate is 16 kHz, and the membrane is of parameters as described in the figures above. The wave speed in the snares is set to 30 m/s.

5 Concluding Remarks

As mentioned in the introduction, this has been a preliminary numerical study of the coupled membrane/snare interaction, embedded in a 3D computational domain. The intention here has been merely to show that such a simulation of a complex system is indeed possible, to exhibit certain features of such a sys-
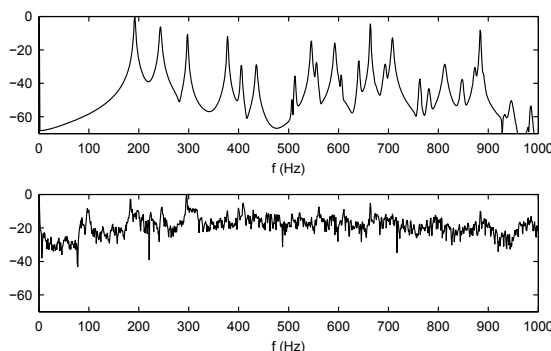
Figure 8: Spectrum of sound output for a coupled membrane system with the snares disengaged (top) and engaged (bottom). System parameters are as in the previous examples.

tem, and to show that such a simulation does not incur an unreasonable computational cost. A necessary step is calibration and validation via experimental measurement. Some of the system parameters, and in particular the geometrical and material properties of the various components are easily determined, but others, such as membrane and snare tension are more difficult to determine, especially in a highly coupled setting. Such work is currently under way at Edinburgh.

Certain features have not been explicitly modelled here—these include effects of stiffness in the membrane and snares, and more importantly, vibration of the drum shell itself, which, though it does not radiate significant energy, is nonetheless capable of storing energy, and may affect the over-all dynamics of the snare drum (particularly with regard to global solution decay). Nonlinear behaviour of the membranes themselves, though it will unquestionably lead to pitch glides when the snare is disengaged, may probably be ignored in the case when the snares are indeed in contact with the membrane. Another question, of more general relevance to 3D modeling of musical instruments, is of the order of the absorbing boundary condition to be applied at the outer faces of the computational domain necessary such that numerical reflections are inaudible—this is a subtle question, because although numerical reflections are typically large at angles of incidence far from the normal, such reflections tend to remain in the region near the boundaries, and may not contaminate the solution as much as might be expected.

Acknowledgements

References

[1] J.-P. Berenger. A perfectly matched layer for the absorption of electromagnetic waves. *Journal of Computational Physics*, 114(2):185–200, October 1994.

[2] J.-P. Berenger. Three-dimensional perfectly matched layer for the absorption of electromag-netic waves. *Journal of Computational Physics*, 127(2):363–379, September 1996.

[3] H. Berger. A new approach to the analysis of large deflections of plates. *Journal of Applied Mathematics*, 22:465–472, 1955.

[4] S. Bilbao. *Numerical Sound Synthesis: Finite Difference Schemes and Simulation in Musical Acoustics.* John Wiley and Sons, Chichester, UK, 2009.

[5] A. Chaigne and A. Askenfelt. Numerical simulations of struck strings. I. A physical model for a struck string using finite difference methods. *Journal of the Acoustical Society of America*, 95(2):1112–1118, 1994.

[6] B. Engquist and A. Majda. Absorbing boundary conditions for the numerical evaluation of waves. *Mathematics of Computation*, 31(139):629–651, 1997.

[7] G. Evans, J. Blackledge, and P. Yardley. *Numerical Methods for Partial Differential Equations.* Springer, London, UK, 1999.

[8] R. Marogna and F. Avanzini. A block-based physical modeling approach to the sound synthesis of drums. Under review, IEEE Transactions on Audio Speech and Language Processing, 2010.

[9] L. Rhaouti, A. Chaigne, and P. Joly. Time-domain modeling and numerical simulation of a kettledrum. *Journal of the Acoustical Society of America*, 105(6):3545–3562, 1999.

[10] T. Rossing, I. Bork, H. Zhao, and D. Fystrom. Acoustics of snare drums. *Journal of the Acoustical Society of America*, 92(1):84–94, 1992.

[11] J. Strikwerda. *Finite Difference Schemes and Partial Differential Equations.* Wadsworth and Brooks/Cole Advanced Books and Software, Pacific Grove, California, 1989.

[12] A. Taflove. *Computational Electrodynamics.* Artech House, Boston, Massachusetts, 1995.

[13] K. Yee. Numerical solution of initial boundary value problems involving Maxwell's equations in isotropic media. *IEEE Transactions on Antennas and Propagation*, 14:302–307, 1966.

[14] S. Zambon, H.-M. Lehtonen, and B. Bank. Simulation of piano sustain-pedal effect by parallel second-order filters. In *Proceedings of the 11th International Digital Audio Effects Conference*, pages 199–204, Espoo, Finland, September 2008.